

Cyclic test for solid steel reinforced concrete frames with special-shaped columns

Zu Q. Liu*, Jian Y. Xue, Hong T. Zhao and Liang Gao

College of Civil Engineering, Xi'an University of Architecture and Technology, Xi'an, China

(Received June 18, 2013, Revised April 21, 2014, Accepted April 23, 2014)

Abstract. An experimental study was performed to investigate the seismic performance of solid steel reinforced concrete (SRC) frames with special-shaped columns that are composed of SRC special-shaped columns and reinforced concrete beams. For this purpose, two models of two-bay and three-story frame, including an edge frame and a middle frame, were designed and tested. The failure process and patterns were observed. The mechanical behaviors such as load-displacement hysteretic loops and skeleton curves, load bearing capacity, drift ratio, ductility, energy dissipation and stiffness degradation of test specimens were analyzed. Test results show that the failure mechanism of solid SRC frame with special-shaped columns is the beam-hinged mechanism, satisfying the seismic design principle of “strong column and weak beam”. The hysteretic loops are plump, the ductility is good and the capacity of energy dissipation is strong, indicating that the solid SRC frame with special-shaped columns has excellent seismic performance, which is better than that of the lattice SRC frame with special-shaped columns. The ultimate elastic-plastic drift ratio is larger than the limit value specified by seismic code, showing the high capacity of collapse resistance. Compared with the edge frame, the middle frame has higher carrying capacity and stronger energy dissipation, but the ductility and speed of stiffness degradation are similar. All these can be helpful to the designation of solid SRC frame with special-shaped columns.

Keywords: solid steel; steel reinforced concrete (SRC); frame with special-shaped columns; cyclic test; seismic behavior

1. Introduction

Steel reinforced concrete (SRC) special-shaped column structure is a new structural system. It not only makes better use of available space and improves the esthetic appearance of structure, which are the superiority of special-shaped column structure (Rammamurthy and Hafeez Khan 1983, Hsu 1989, Sinha 1996, Balaji and Murty 2001a, Wang *et al* 2010), but also has high load bearing capacity and good seismic performance, which are the merit of SRC structure (Shim *et al* 2008, Ellobody and Yong 2011a, Kim *et al* 2012a). So, SRC special-shaped column structure has become a popular research topic in many scientific institutes (Zhou 2012b, Kim 2011b).

At present, researches about SRC special-shaped column structure mainly focus on the basic mechanical behaviors and seismic performance of members and joints (Tokgoz and Dundar 2012c,

*Corresponding author, Ph. D., E-mail: liuzuqiang0081@126.com

Li *et al* 2007a, Xu *et al* 2009a, Chen *et al* 2007b, Xue *et al* 2012d, Xiang 2006, Xue *et al* 2009b). However, few have been done on structural system. In 2009, a 1/2 scale model of one-bay and two-story frame composed of lattice SRC T-shaped section columns and reinforced concrete (RC) beams was performed by the pseudo-dynamic and pseudo-static tests (Yang and Zhang 2009c), and the results showed that it had good ductility and energy dissipation capacity. But the specimen was not the typical form of SRC frame with special-shaped columns, so it didn't reveal the mechanical performance of the new frame comprehensively.

There are two typical forms of SRC frame with special-shaped columns, including the edge frame and the middle frame. In the edge frame, L-shaped column is as corner column, and T-shaped column is as side column. In the middle frame, T-shaped column is as side column, and \boxplus -shaped column is as middle column (Fig. 1). In this paper, according to the two typical forms mentioned above, two specimens were designed and tested under low reversed cyclic loading. The mechanical behaviors were obtained and analyzed, which could be helpful for popularizing the new structural system.

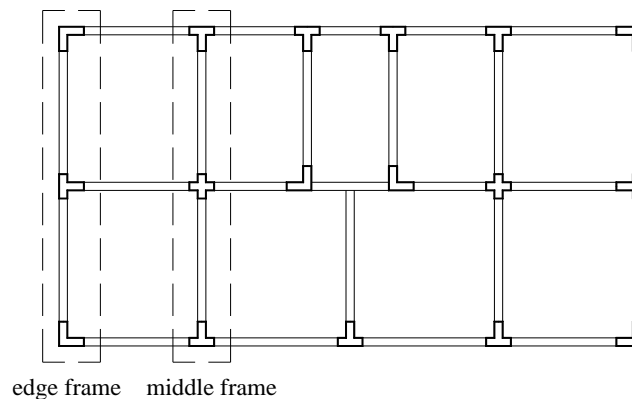
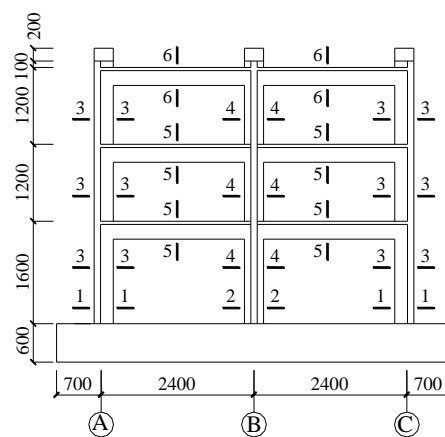
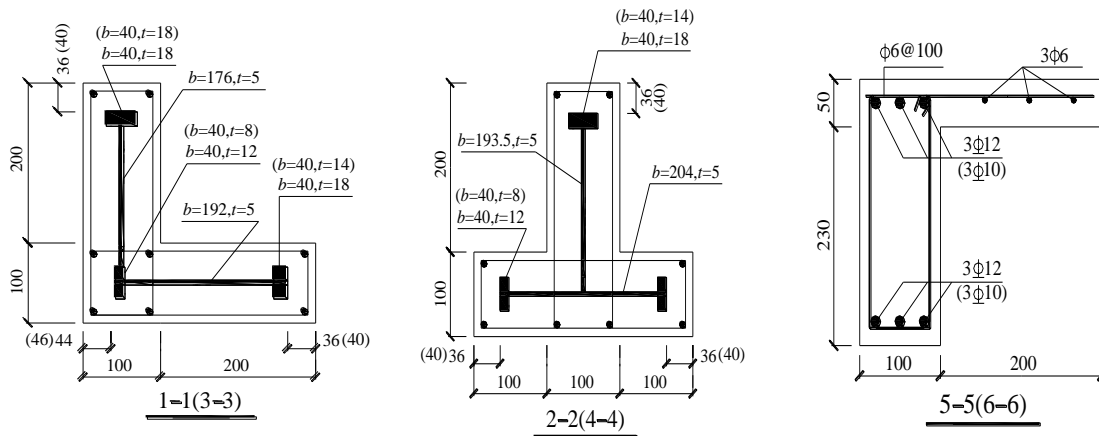


Fig.1 Plan of SRC frame with special-shaped columns

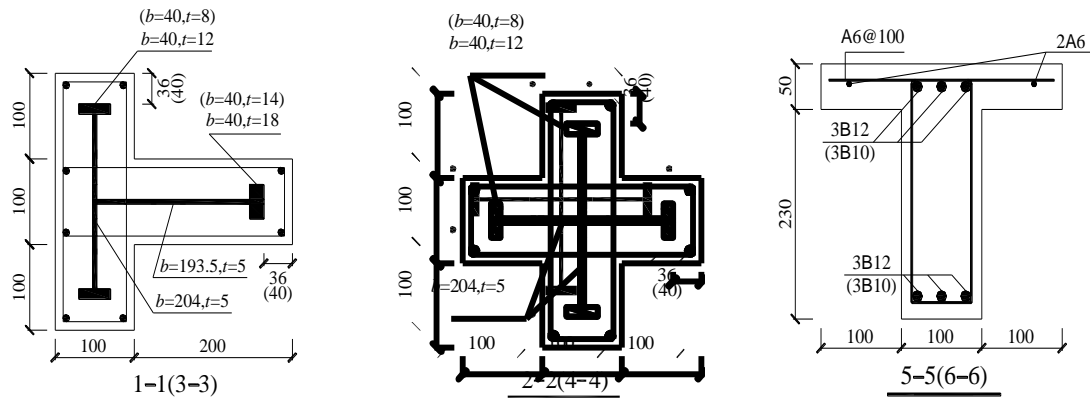


(a) Frame model

Fig. 2 Continued



(b) Sections of columns and beams of SYBK



(c) Sections of columns and beams of SYZK

Fig. 2 Geometry and steel layout of the test specimens

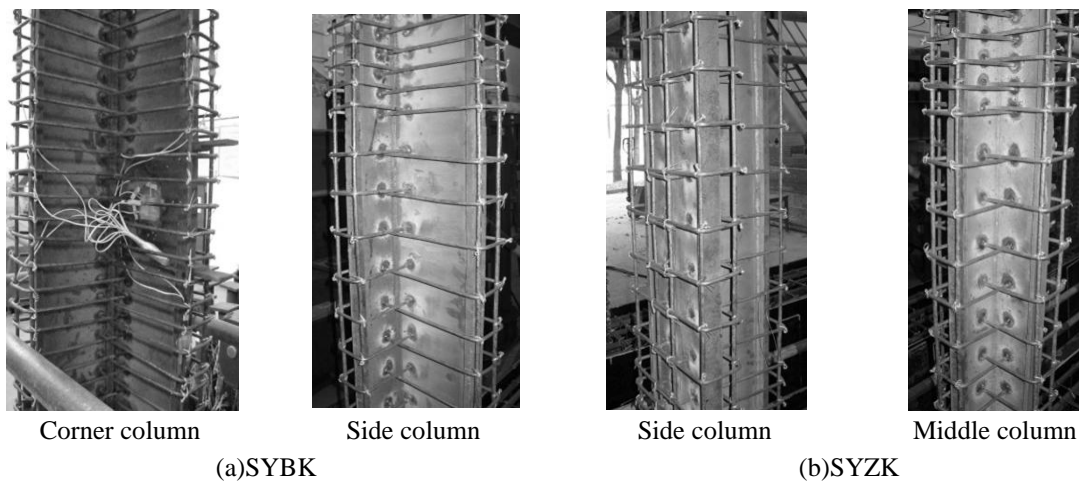


Fig.3 Steel skeleton

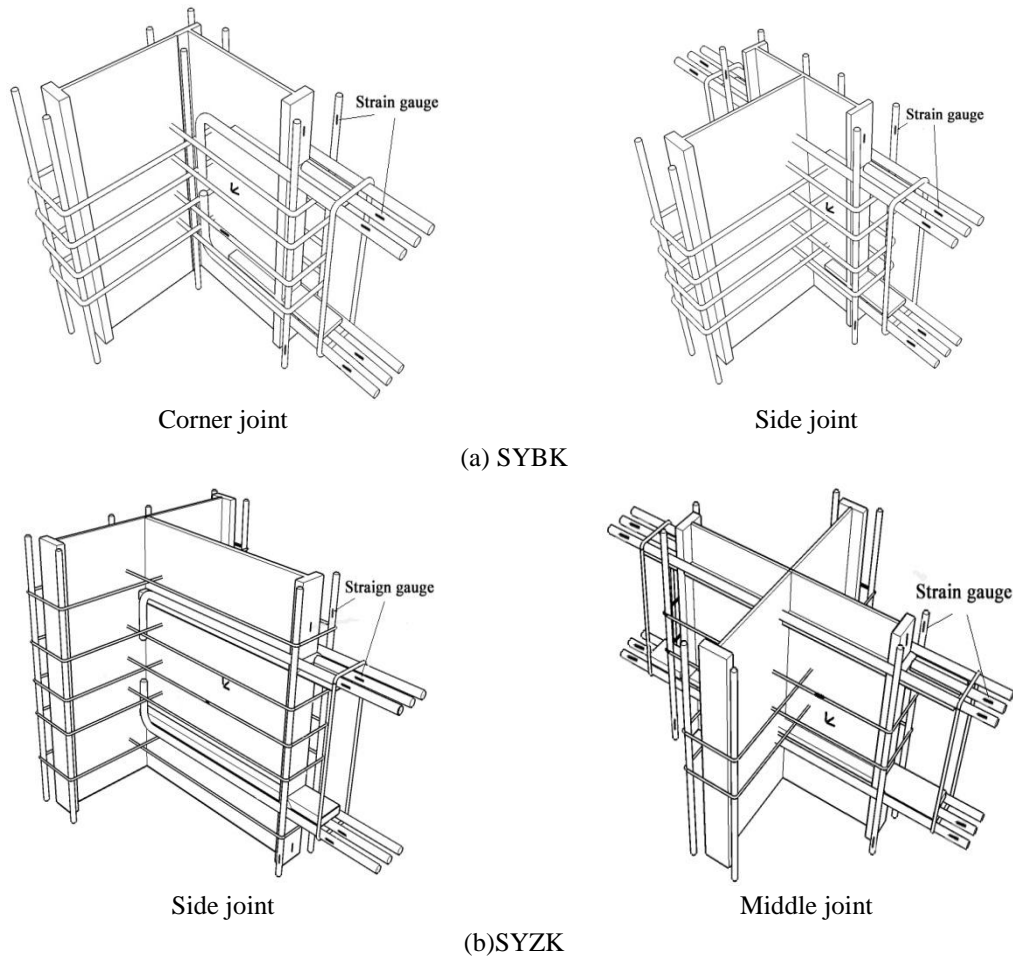
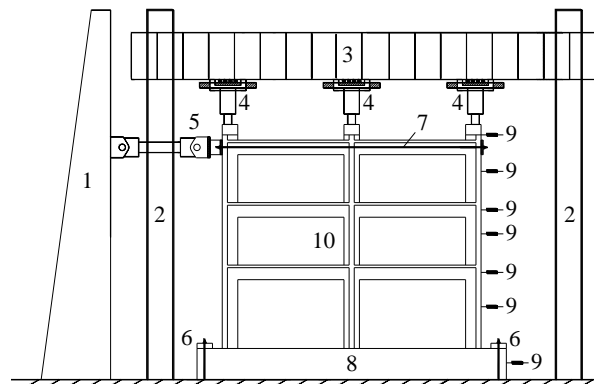


Fig. 4 Details of joints



1 reaction wall. 2 reaction steel frame. 3 reaction girder. 4 vertical actuator. 5 1000kN horizontal actuator. 6 tie bolt. 7 horizontal braces. 8 footing. 9 displacement transducer. 10 test specimen

Fig. 5 Test setup and instrumentation

Table 1 Properties of reinforcements and steel plates

Material	Diameter (Plate thickness)	Yield strength f_y (MPa)	Ultimate strength f_u (MPa)	Elastic modulus E_s (MPa)
Reinforcement	A6	302.3	442.7	2.24×10^5
	A8	320.7	472.7	2.36×10^5
	B10	439.0	654.0	1.95×10^5
	B12	406.3	597.3	1.92×10^5
Steel plate	5 mm	367.1	471.3	2.13×10^5
	8 mm	323.8	459.9	1.93×10^5
	12 mm	471.5	605.7	2.10×10^5
	14 mm	316.4	471.9	2.11×10^5
	18 mm	302.9	465.0	1.72×10^5

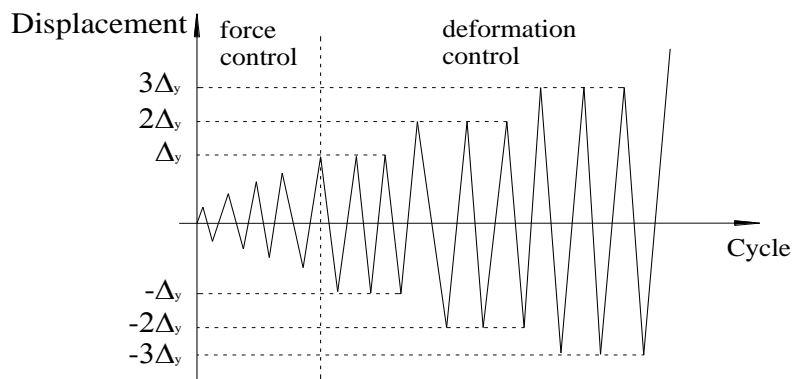


Fig.6 Loading control process

2. Specimens and test setup

According to the principle of “strong column and weak beam” and “strong joint and weak member”, two specimens, SYBK and SYZK, were designed as 1/2.5 scale models of two-bay and three-story frame, which were composed of solid SRC special-shaped columns and RC beams. SYBK was the edge frame, and SYZK was the middle frame. The geometry and steel layout of the specimens are shown in Fig. 2, in which all the dimensions are in millimeter.

The height and thickness of column limb were respectively 300 mm and 100 mm, the ratio between which was 3. The steel skeletons (Fig. 3), which were inside columns, were manufactured through three steps. The first step was that the steel plates were welded into the integral steel with definite shape; the second step was that the stirrups were formed to the U-shaped or the closed rectangular-shaped and then welded on the integral steel; and the last step was that the longitudinal reinforcement was assembled with the stirrups. In order to consider the effects of floor slab, the inverted L-shaped beams and the T-shaped beams were respectively adopted in SYBK and SYZK.

B8 bars were used as longitudinal reinforcements in columns, and A6 bars were used as stirrups in columns and beams, the interval of which was 40 mm at intensive area and 80 mm at non-intensive area. At the joint area (Fig. 4), the corner reinforcements of the beam passed through the sides of steel skeleton of the column, and were anchored with concrete, and the middle

reinforcement was welded to the junction plate, which was the part of steel skeleton.

Fine aggregate commercial concrete was used to pour test specimens. The cubic concrete compressive strength measured at the 28th day was 26.95MPa for SYBK and 31.22MPa for SYZK. Properties of reinforcements and steel plates are shown in Table 1.

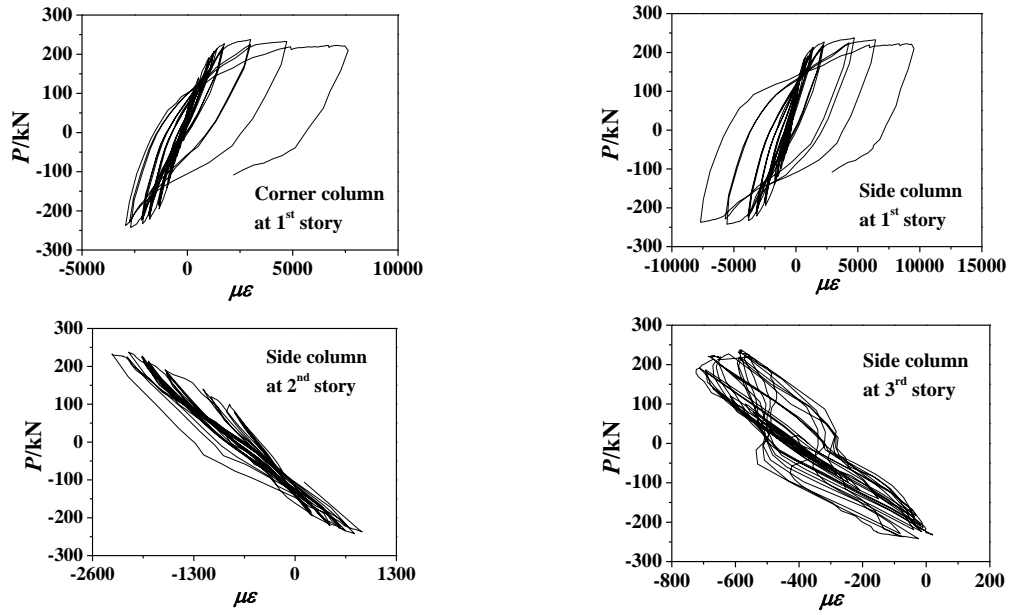
The test setup and instrumentation are shown in Fig. 5. The axial loads were exerted by three vertical actuators on the top of each column of test specimen. For SYBK, 281.2kN force was loaded at the corner column, and 562.4kN force was loaded at the side column; for SYZK, 277.5kN force was loaded at the side column, and 555.0kN force was loaded at the middle column. Lateral low cyclic reversed load was applied at the top beam end by horizontal actuator, which was controlled by MTS electro-hydraulic servosystem. Strain gages were mounted at critical positions of the steels, longitudinal reinforcements and stirrups to measure the strain history during the test (Fig. 4). Lateral displacements at each story were measured by displacement transducers (LVDTs) (Fig. 5). All data was collected by TDS-602 static data acquisition instrument.

Load-displacement hybrid control program was applied, which means the lateral loading sequence was controlled by force for the initial loading cycles till test specimens were observed starting to yield. This observation was accomplished by monitoring the reaction forces of the MTS horizontal actuator. At the initial loading phase, every load level increased 20 ~ 30kN and circulated 1 cycle. When the test specimen was observed becoming yield, the loading sequence was controlled by displacement. On the basis of the yield displacement, the target displacements for the cyclic loading were set as the multiple of the yield displacement(Δ_y), and the cyclic loadings were repeated three times at each target displacement, and stopped until the reaction force descended to about 85% of the maximum value or the displacement exceeded the maximum displacement of the test setup. The loading process is shown in Fig. 6. During the test, the load/displacement was stopped at several “load stage” so that the data could be taken by acquisition instrument, cracks marked, crack width measured, and pictures taken.

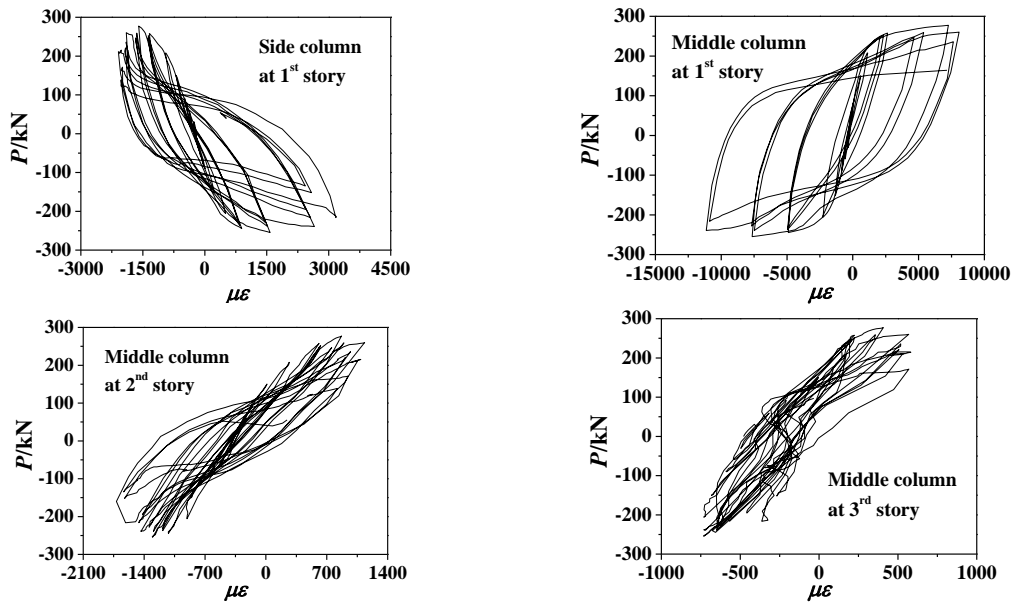
3. Test results

3.1 Failure characteristic

For SYBK and SYZK, the failure patterns are very similar. The damage of test specimens happened at beam ends firstly, and cracks mainly distributed at the 1/3 area of each beam end. When specimens failed, the main flexural cracks formed at each beam end, and few shear cracks developed. The longitudinal reinforcements of beams yielded early and plastic hinges developed at all beam ends. For the columns, damage was concentrated at the bottom ends of first-story columns and the top end of third-story side column (in SYBK) or middle column (in SYZK). At these positions, steel plates yielded and plastic hinges developed. There was no plastic hinge developing at other column ends. At the same time, the columns indicated good shear performance because of the solid steel, and there were few shear cracks along the height of columns. Damage happened slightly and finally at the beam-column joints. Shear failure didn't occur at the panel zones and steel plates didn't yield. Principal strains of steel plates at bottom ends of columns and panel zones are shown in Fig. 7 and Fig. 8 respectively, and the failure patterns of test specimens are shown in Fig. 9, Fig. 10 and Fig. 11.



(a) SYBK



(b) SYZK

Fig.7 Principal strains of steel plates at bottom end of columns

The subsequence of plastic hinges of the test specimens are shown in Fig. 12, in which positive and negative direction represents the push and pull direction of loading respectively. From the figure, it is seen that the failure mechanism of the test specimens is the beam-hinged mechanism, satisfying the seismic design principle of “strong column and weak beam”.

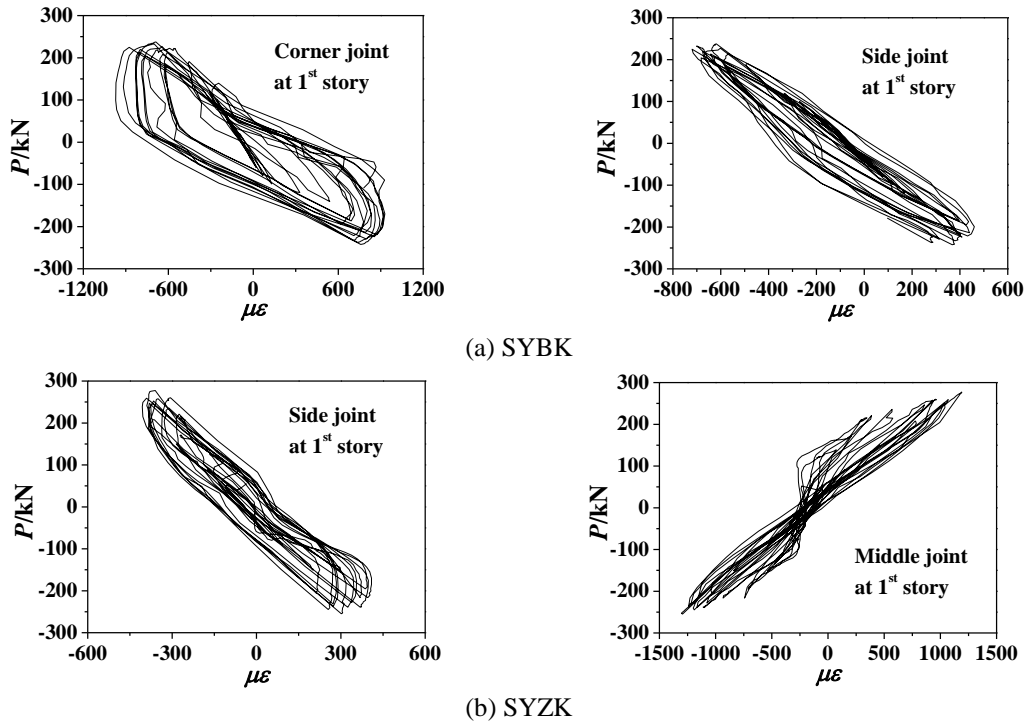


Fig.8 Principal strains of steel plates at panel zones



Fig.9 Failure patterns of whole frames

3.2 Lateral load-displacement relationship

Fig. 13 shows the lateral load-top displacement hysteretic loops obtained from test. From the figure, it is showed that SYBK and SYZK, columns of which were reinforced by solid steel, display good hysteretic performance. Hysteretic loops are full and approximately symmetric, which are in shuttle or bow shape. For SYBK, the last target displacement was applied at the

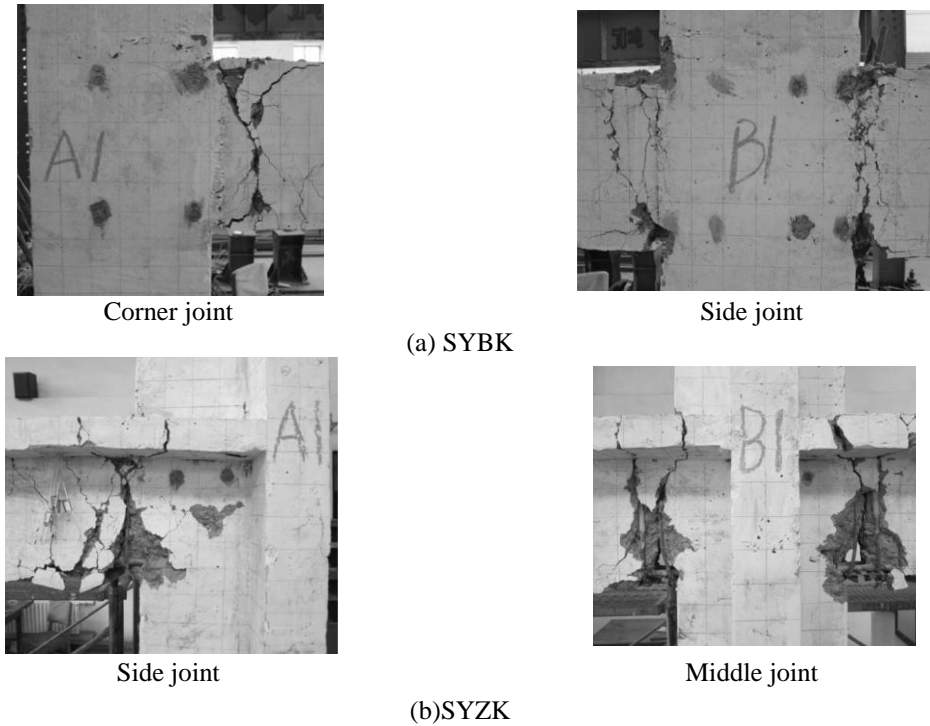


Fig.10 Failure patterns of beam-column joints

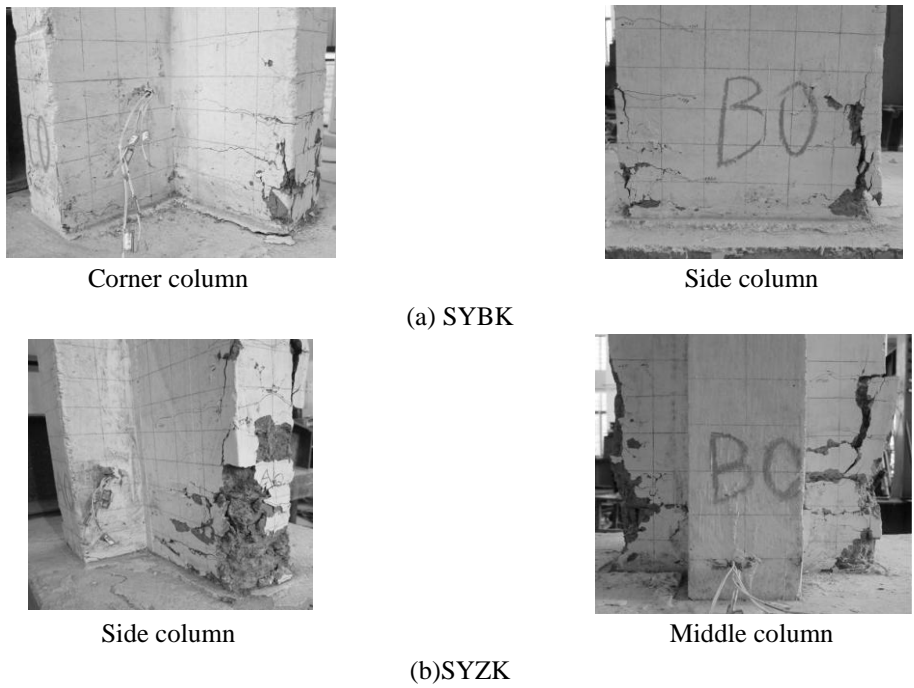


Fig.11 Failure patterns of column roots

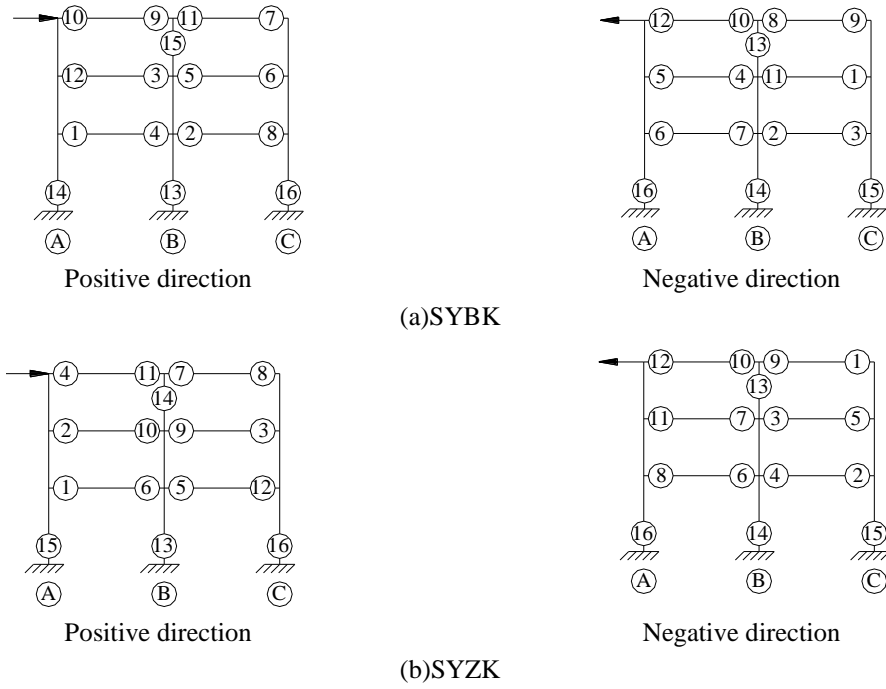


Fig. 12 Subsequence of plastic hinges of specimens

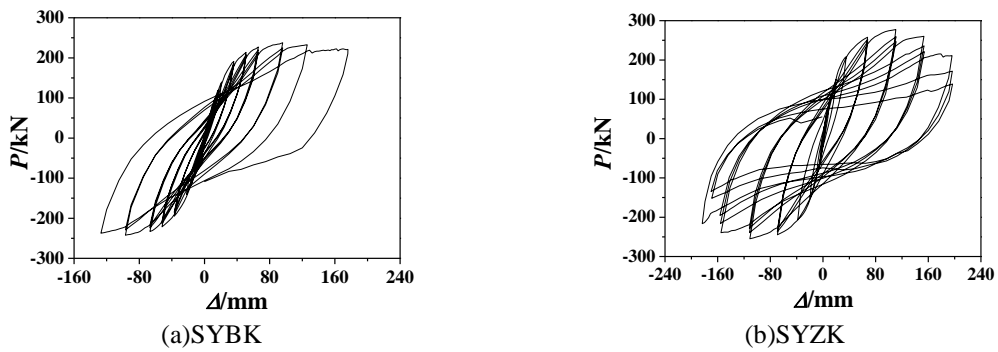


Fig.13 Hysteretic loops of test specimens

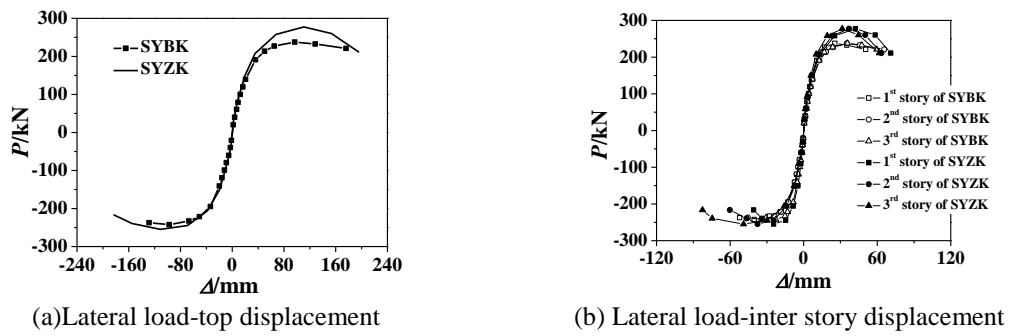


Fig.14 Skeleton curves

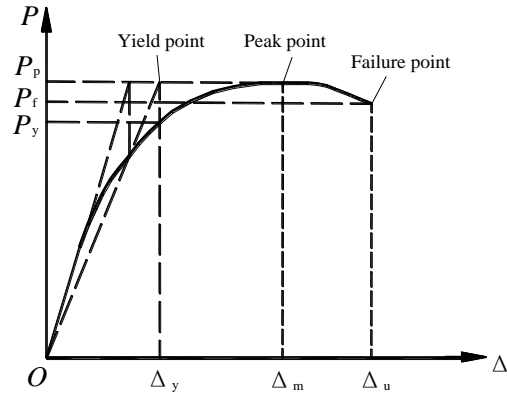


Fig.15 Method of universal yield moment

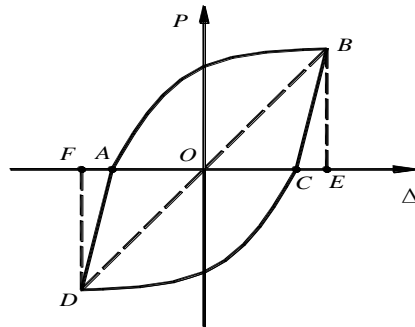
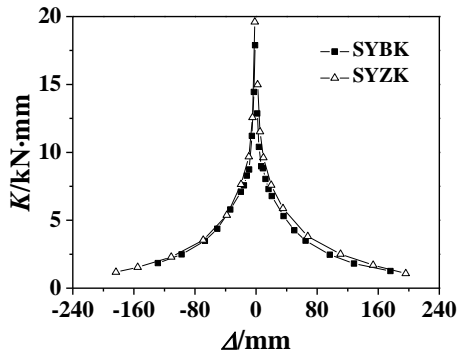
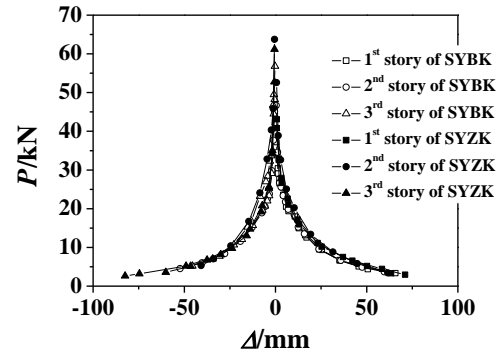


Fig.16 Calculation of equivalent viscous damping coefficient



(a) Integral stiffness



(b) Inter-story stiffness

Fig.17 Curves of stiffness degradation

Table 3 Displacement ductility coefficients

Specimen	Integrity		1 st story		2 nd story		3 rd story	
	Positive	Negative	Positive	Negative	Positive	Negative	Positive	Negative
SYBK	5.3	—	5.1	—	5.5	—	5.1	—
SYZK	4.9	6.1	4.9	6.0	4.7	4.5	5.2	7.5
KYZK	4.3	4.6	4.4	4.2	4.1	4.4	4.4	4.4

Table 4 Equivalent viscous damping coefficients of specimens

Specimen	h_e		
	Yield point	Peak point	Failure point
SYBK	0.091	0.173	0.240
SYZK	0.110	0.202	0.249
KYZK	0.078	0.172	0.212

positive direction only, which resulted in the hysteretic loops showing asymmetry. But before the last “load stage”, the hysteretic loops are symmetry.

Fig. 14(a) compares the skeleton curves of lateral load and top displacement for both specimens. It shows that the load bearing capacity of SYZK is greater than that of SYBK. This is because when the lateral load was applied to SYBK, the action line of load didn't pass the axis of section figure center of special-shaped columns and beams, which resulted in the whole frame and special-shaped columns torsion. So the steels inside of columns were not sufficiently used, and the load bearing capacity was reduced. However, the action line of lateral load passed the axis of section figure center of special-shaped columns and beams justly for SYKY, and the steels were made full use of. So its load bearing capacity is greater. At the same time, it shows that the descending branch of curve of SYZK is steeper than that of SYBK at positive direction, but there was no significantly difference at negative direction. Fig. 14(b) compares the skeleton curves of lateral load and inter-story displacement.

The test results at the yield point, peak point and failure point of specimens were summarized in Table 2. The definition of the yield point (P_y , Δ_y) was on the basis of the method of universal yield moment, the process of which is showed in Fig. 15 (Yao and Chen 2001b). The failure point (P_f , Δ_f) was defined as the point corresponding to 85% of the load of peak point (P_p). θ stands for the drift ratio, which is defined as Δ/H , where Δ stands for the top or inter-story displacement, and H stands for the whole or story height. When the loading stops, the load of SYBK didn't descend to 85% of P_p . So P_f of SYBK is defined as the load corresponding to the maximum displacement at positive direction, which is 93% of P_p .

As shown in Table 2, the integral drift ratio and inter-story drift ratio of test specimens were respectively much larger than the limit value of reinforced concrete frame specified by Chinese seismic design code, which is equal to 1/50, indicating that test specimens have a high level of collapse resistance.

3.3 Displacement ductility

Displacement ductility is an important performance for structure, which can reflect if the structure has excellent plastic deformation capacity. Displacement ductility is usually represented by displacement ductility coefficient, which was defined as Δ_f/Δ_y . The displacement ductility coefficients obtained from test are shown in Table 3. At the same time, the displacement ductility coefficients of a lattice STC frame with special-shaped columns (KYZK) are listed (Xue *et al* 2012e). It is shown that the positive integral displacement ductility coefficient of SYBK (5.3) is approximately equal to the average of integral displacement ductility coefficients in positive and negative directions (5.5), which shows that the edge frame and the middle frame with SRC special-shaped columns have the same displacement ductility, which is good. The both are larger

than the average of KYZK (4.45). It is indicated that the displacement ductility of solid SRC frame with special-shaped columns is better than that of the lattice SRC frame with special-shaped. The similar conclusion can be obtained from the inter-story displacement ductility coefficients too.

3.4 Energy dissipation capacity

Energy dissipation capacity is an important seismic performance index for structure, which is usually represented by equivalent viscous damping coefficient h_e . By analyzing the hysteretic loops of test specimens under low cyclic reversed loading, the degree of energy dissipation under different loading level can be investigated. The equivalent viscous damping coefficient can be written as follows:

$$h_e = \frac{1}{2\pi} \cdot \frac{S_{(ABCD A)}}{S_{(OBE+ODF)}} \quad (1)$$

where $S_{(ABCD A)}$ and $S_{(OBE+ODF)}$ represents the area of hysteretic loop ABCDA and triangles OBE and ODF respectively, which are showed in Fig. 16. The calculated results of test specimens are listed in Table 4, in which h_{ey} , h_{ep} and h_{ef} stands for the equivalent viscous damping coefficient at yield, peak and failure point respectively. The relevant coefficients of KYZK are listed too (Xue 2012). It is shown that at yield point and peak point, the energy dissipation capacity of SYZK is much better than that of SYBK, but at failure point, there is no significant difference between SYZK and SYBK. Compared with the lattice SRC frame with special-shaped columns, the solid SRC frame with special-shaped columns indicates excellent energy dissipation capacity, and at failure point, the equivalent viscous damping coefficient of SYBK and SYZK was 1.132 and 1.175 times that of KYZK, respectively.

3.5 Stiffness

Stiffness of test specimens under low cyclic reversed loading can be expressed in the way of secant stiffness that is the ratio between the positive or negative maximum load and the corresponding displacement at every loading cycle. As the top displacement increasing, the stiffness of specimens degrades gradually, which is defined as stiffness degradation. The integral and inter-story stiffness degradation of test specimens under different loading level are shown in Fig. 17. Fig. 17(a) shows that the stiffness of SYBK and SYZK is similar. The initial stiffness of both specimens in positive and negative direction is not equivalent. This may be because the asymmetry of structure, which resulted from the deviation of manufacturing process. As the top displacement increasing, the positive and negative stiffness of specimens approach gradually. Before test specimens were observed yielding, a lot of concrete cracks occurred which led to a fast stiffness degradation, and with the development of plastic deformation, the stiffness degradation slowed down gradually. Fig. 17(b) shows that the inter-story stiffness degradation has the same regulation with integral stiffness degradation, and the speed of degradation is from fast to slow. For SYBK or SYZK, each inter-story displacement in positive and negative direction was approximately the same, indicating that the test specimen has uniform vertical stiffness, and there is no obvious weak story. Although the first-story height is larger than the other two stories, reinforcement of steels had been applied to the first-story column ends. Therefore, test specimens have uniform vertical stiffness in the whole loading process.

4. Conclusions

An experimental study was performed to investigate the structural performance of solid SRC frames with special-shaped columns, which were subjected to low cyclic reversed loading. For comparison, two solid SRC frames with special-shaped columns were designed and tested, including an edge frame and a middle frame. Test phenomenon and results were analyzed, and the findings of the present experimental studies are summarized as follows:

- The solid SRC frame with special-shaped columns is a typical structure of “strong column and weak beam”. During the loading process, plastic hinges firstly occurred at beam ends, and then occurred at column ends, and the failure mechanism of test specimens were the beam- hinged mechanism.
- The hysteretic loops of test specimens were plump, and the ductility and the energy dissipation capacity were good. The seismic performance of the solid SRC frame with special-shaped columns is more excellent than that of the lattice SRC frame with special-shaped columns.
- The test specimens showed good capacity of collapse resistance, and the ultimate integral drift ratio of SYBK was 1/23 and of SYZK was 1/22. The stiffness degraded with the top displacement increasing, and the speed of stiffness degradation was from fast to slow.
- Compared with the edge frame, the bearing capacity of the middle frame is greater, and the energy dissipation capacity is stronger. However, the ductility and the speed of stiffness degradation of the both are similar.

Acknowledgments

The authors would like to thank the Natural Science Foundation of China (Granted No.50978384 and 51308444), Doctoral Fund of Ministry of Education of China (Granted No. 20096120110005), Scientific Research Plan Project of Shaanxi Education Department (Granted No.2013JK0979) and Program for Innovation Team of Xi'an University of Architecture and Technology for their supports of this study.

References

- Rammamurthy, L.N. and Hafeez Khan, T.A. (1983), “L-shaped column design for biaxial eccentricity”, *J. Struct. Eng.*, **109**(8), 1903-1917.
- Hsu, Cheng-Tzu Thomas (1989), “T-shaped reinforced concrete members under biaxial bending and axial compression”, *ACI Struct. J.*, **86**(4), 460-468.
- Sinha, S.N.(1996), “Design of cross (+) section of column”, *The Indian Concrete J.*, **70**(3), 153-158.
- Balaji, K.V.G.D. and Murty, D.S.R. (2001a), “Reliability analysis of RC T-shaped column sections”, *Indian Concrete J.*, **75**(3), 223-227.
- Wang, T.C., Zhang, X.H., Zhao, H.L. and Qi, J.W. (2010), “Experimental research on seismic behavior of exterior joints with specially shaped columns reinforced by fiber”, *Indus. Construct.*, **40**(1), 46-50.
- Shim, C.S., Chung, Y.S. and Han, J.H. (2008), “Cyclic response of concrete-encased composite columns with low steel ratio”, *Proceedings of the Institution of Civil Engineers: Struct. Build.*, **161**(2), 77-89.
- Ellobody, E. and Yong, B. (2011a), “Numerical simulation of concrete encased steel composite columns”, *J. Construct. Steel Res.*, **67**(2), 211-222.

- Kim, C.S., Park, H.G. and Chung, K.S. (2012a), "Eccentric axial load testing for concrete-encased steel columns using 800MPa steel and 100MPa Concrete", *J. Struct. Eng.* **138**(8), 1019-1031.
- Zhou, T., Chen, Z.H. and Liu, H.B. (2012b), "Seismic behavior of special shaped column composed of filled steel tubes", *J. Construct. Steel Res.*, **75**: 131-141.
- Kim, S.H., Jung, C.Y. and Ann, J.H. (2011b), "Ultimate strength of composite structure with different degrees of shear connection", *Steel Compos. Struct.*, **11**(5), 375-390.
- Tokgoz, S. and Dundar, C. (2012c), "Test of eccentrically loaded L-shaped section steel fibre high strength reinforced concrete and composite columns", *Eng. Struct.*, **38**(5): 134-141.
- Li, Z., Zhang, X.F., Guo, Z.Y. and Xu, K. (2007a), "Experimental study on the mechanical property of steel reinforced concrete short columns of t-shaped cross-section", *China Civil Eng. J.*, **40**(1), 1-5.
- Xu, Y.F., Diao, X.Z., Guo, J., Wang, C.C., Li, X.L. and Wang, H. (2009a), "Experimental study on the biaxial eccentric pressure bearing capacity of cross-shaped steel reinforced concrete columns", *J. Shenyang Jianzhu Univ. (Natural Science)*, **25**(1), 100-105.
- Chen, Z.P., Xue, J.Y., Zhao, H.T., Shao, Y.J. Zhao, Y.H. and Men, J.J. (2007b), "Experimental research on seismic behavior of steel reinforced concrete special-shaped columns", *J. Build. Struct.*, **28**(3), 53-61.
- Xue, J.Y., Chen, Z.P., Zhao, H.T., Gao, L. and Liu, Z.Q. (2012d), "Shear mechanism and bearing capacity calculation on steel reinforced concrete special-shaped columns", *Steel Compos. Struct.*, **13**(5), 473-487.
- Xiang, P. (2006), "Experimental research on joints of steel reinforced concrete special-shaped column and reinforced concrete beam under double-direction low-cyclic reversed loading", Master Dissertation, Guangxi University, Nanning, China.
- Xue, J.Y., Liu, Y., Zhao, H.T., Chen, Z.P. and Sui, Y. (2009b), "Experimental study on seismic behavior of steel reinforced concrete special-shaped column-beam joints", *J. Build. Struct.*, **30**(4), 69-77.
- Yang, T. and Zhang, X.D. (2009c), "Research on seismic behavior of frame with T-shaped SRC columns", *J. Civil, Architect. Environ. Eng.*, **31**(2), 33-37.
- Yao, Q.F. and Chen, P. (2001b), *Civil Engineering Structure Test*, China Architecture & Building Press, Beijing, China.
- Xue, J.Y., Gao, L., Liu, Z.Q., Zhao, H.T. and Ge, H.P. (2012e), "Quasi-static test and finite element analysis on lattice steel reinforced concrete middle frame with special-shaped columns", *J. Build. Struct.*, **33**(8), 31-40.